AD-A186 235 HIGH MIDPLANE ACCESSIBILITY STELLARATOR WINDINGS FOR HIGH CURRENT TOROIDAL ACCELERATORS(U) NAVAL RESEARCH LAB WASHINGTON DC S J MARSH ET AL. 06 OCT 87 1/1

UNCLASSIFIED NRL-MR-6025 F/G / NL

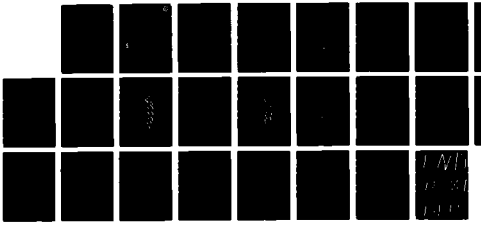

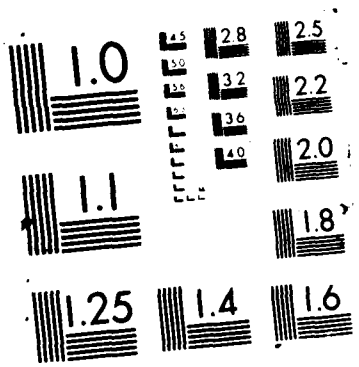
1.0
1.1
1.25
1.4
1.6
1.8
2.0
2.2
2.5
2.8
3.2
3.6
4.0
4.5
5.0
5.6

Naval Research Laboratory

Washington, DC 20375-5000

NRL Memorandum Report 6025

High Midplane Accessibility Stellarator Windings for High Current Toroidal Accelerators

S. J. MARSH,* J. GOLDEN, AND C. A. KAPETANAKOS

Plasma Physics Division

D. ANDERSON

Omicron Technology, Inc.
Madison, Wisconsin 53705

**Sachs/Freeman Associates*
Landover, MD 20785

October 6, 1987

This work was supported Spawar 11-4, PMW 145P and by ONR.

SECURITY CLASSIFICATION OF THIS PAGE

REPORT DOCUMENTATION PAGE

1a. REPORT SECURITY CLASSIFICATION UNCLASSIFIED	1b RESTRICTIVE MARKINGS
2a. SECURITY CLASSIFICATION AUTHORITY	3. DISTRIBUTION / AVAILABILITY OF REPORT Approved for public release; distribution unlimited.
2b. DECLASSIFICATION / DOWNGRADING SCHEDULE	
4. PERFORMING ORGANIZATION REPORT NUMBER(S) NRL Memorandum Report 6025	5. MONITORING ORGANIZATION REPORT NUMBER(S)
6a. NAME OF PERFORMING ORGANIZATION Naval Research Laboratory 6b. OFFICE SYMBOL (If applicable)	7a. NAME OF MONITORING ORGANIZATION
6c. ADDRESS (City, State, and ZIP Code) Washington, DC 20375-5000	7b. ADDRESS (City, State, and ZIP Code)
8a. NAME OF FUNDING / SPONSORING ORGANIZATION 8b. OFFICE SYMBOL (If applicable)	9. PROCUREMENT INSTRUMENT IDENTIFICATION NUMBER
8c. ADDRESS (City, State, and ZIP Code)	10. SOURCE OF FUNDING NUMBERS PROGRAM ELEMENT NO. / PROJECT NO. / TASK NO / WORK UNIT ACCESSION NO.

11. TITLE (Include Security Classification)
High Midplane Accessibility Stellarator Windings for High Current Toroidal Accelerators

12. PERSONAL AUTHOR(S)
Marsh, S. J.,* Golden, J., Kapetanakos, C. A., and Anderson, D.**

13a. TYPE OF REPORT	13b. TIME COVERED FROM _____ TO _____	14. DATE OF REPORT (Year, Month, Day)	15. PAGE COUNT
		1987 October 6	35

16. SUPPLEMENTARY NOTATION
This work was supported by Spawar 11-4, PMW 145P and ONR. (See page ii)

17. COSATI CODES			18. SUBJECT TERMS (Continue on reverse if necessary and identify by block number)
FIELD	GROUP	SUB-GROUP	Accelerators Modified betatron Strong focusing

19. ABSTRACT (Continue on reverse if necessary and identify by block number)

We have developed two strong focusing field configurations that provide high midplane accessibility and therefore are compatible with presently contemplated extraction schemes for high current, toroidal accelerators. When these windings are attached to a modified betatron accelerator, the bandwidth of the device is slightly smaller than the bandwidth of a modified betatron with unsplit stellarator windings. However, the bandwidth of the two new configurations is more than sufficient even for modest (20-30 kA) winding current.

20 DISTRIBUTION / AVAILABILITY OF ABSTRACT	21 ABSTRACT SECURITY CLASSIFICATION
☒ UNCLASSIFIED/UNLIMITED ☐ SAME AS RPT ☐ DTIC USERS	UNCLASSIFIED
22a NAME OF RESPONSIBLE INDIVIDUAL	22b TELEPHONE (Include Area Code) / 22c OFFICE SYMBOL

DD FORM 1473, 84 MAR 83 APR edition may be used until exhausted
All other editions are obsolete

SECURITY CLASSIFICATION OF THIS PAGE

*U.S. Government Printing Office: 1986—607-047

16. SUPPLEMENTARY NOTATION

*Sachs/Freeman Associates, Landover, MD 20785
**Omicron Technology, Inc., Madison, Wisconsin 53705

CONTENTS

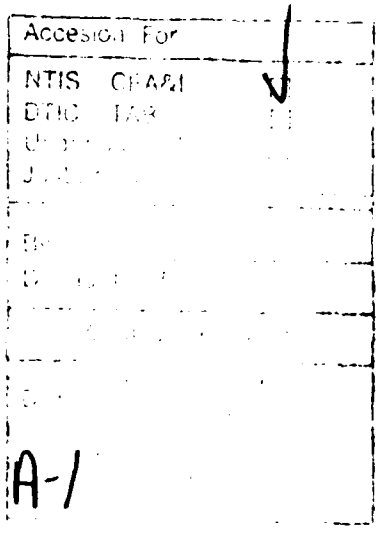

HIGH MIDPLANE ACCESSIBILITY STELLARATOR WINDINGS FOR HIGH CURRENT TOROIDAL ACCELRATORS

I. Introduction

Stability analysis of the electron ring orbits, over the last few years, has shown that the confining properties of the modified betatron accelerator[1-8] can be substantially improved by adding strong focusing[9-11] windings that carry modest current.

The windings that generate the strong focusing field, with poloidal multiplicity l=2, can be either of the stellarator[9] type, i.e., four twisted wires with the current in adjacent wires flowing in opposite directions or of the torsatron[10,11] type, in which two twisted wires carry current in the same direction.

While improving the confining properties of the device, the strong focusing field makes the injection and trapping as well as the extraction of the beam from the magnetic field configuration substantially more involved.

Recently, two injection schemes[10,12] have been developed for toroidal accelerators with strong focusing. In this paper we propose two modified stellarator winding configurations that provide very high midplane accessibility and therefore are compatible with the presently contemplated radial extraction schemes.

Figure 1a shows a three period stellarator winding in the toroidal angle θ, poloidal angle ϕ plane. By cutting these windings near $\phi=0$ and $\phi=2\pi$ and connecting them as shown in Fig. 1b, we obtain a configuration with the current flowing continuously through all the windings as well as the various jumpers that connect them. The parasitic fields generated by

Manuscript approved May 29, 1987.

the jumpers are substantially reduced by two windbacks that run along the j. s and carry half the current of the main windings. In an actual de. ce the proposed split winding continuous stellarator configuration will look as shown in Fig. 2.

In the second, the modular, high midplane accessibility stellarator configuration the windings are cut again near $\phi=0$ and $\phi=2\pi$ but are connected as shown in Fig. 3b. It should be noticed that the direction of the current in the jumpers that are located near $\phi=0$ is opposite to the direction of the current in the jumpers that are located near $\phi=2\pi$. This provides partial cancellation of the parasitic fields generated by the jumpers. Further reduction of the parasitic fields is obtained by two windbacks that run along the jumpers and carry current in the opposite direction. The magnitude of the current in each windback is one half of the current in the windings. In an actual device the proposed modular split winding stellarator configuration will look as shown in Fig. 4.

Although the two configurations appear to be substantially different, careful examination of Figures 2 and 4 reveal that then the windbacks are included, both the magnitude as well as the direction of the current are identical in the two systems. This conclusion is also supported by the numerical studies of the ring dynamics in these two configurations. These studies have shown the ring orbits are identical when the various parameters of the two systems are selected to be the same.

II. Numerical Results

To determine the beneficial effect of these two split winding stellarator configurations on the confining properties of the modified betatron, we have carried out extensive numerical studies of the ring dynamics for a wide range of initial conditions. These studies have mainly focused on the transverse macroscopic electron ring orbits. A typical transverse electron ring orbit is shown in Fig. 5. A measure of the bandwidth of the device is the parameter δ that is defined as the distance from the injection position (106 cm for all the data presented in this report) to the point where the beam orbit crosses the midplane ($z=0$). Since δ is measured from the injection position, its value is negative when the ring orbit crosses the midplane between the inner wall of the torus and the injection position. For an injection position at 106 cm in a 100 cm major radius chamber, we define the "useful bandwidth" as the range of the vertical magnetic field B_z low which δ is between 0 and δ_{max}, where δ_{max} = inner wall torus radius + minor beam radius-injection position. Those orbits that cross the $z=0$ plane between the injection position and the outer wall of the torus are not of interest because the rings that move along these orbits cannot be moved near the minor axis without suffering severe losses on the injector.

To benchmark our results, we initially studied the variation of δ with B_z in a modified betatron with unsplit (regular) stellarator windings for

four different winding currents. The macroscopic ring orbits have been obtained from the numerical integration of the equations of motion. The magnetic fields of the stellarator type windings have been calculated from the Biot-Savart law using filaments of infinitesimal radius. The continuous helical filaments and jumpers are approximated by a series of discrete segments, the number of which can be adjusted. The results for a four winding period stellarator (eight field period) are shown in Fig. 6. The values of the various parameters for this figure are listed in Table I. It is apparent from these results that as the current through the windings increases, the curve rotates counterclock-wise. For the lowest two winding currents (0 and 10kA) the slope of the curve is positive. This is exactly as expected for a space charge dominated electron ring.

It has been shown previously that near the minor axis of the torus the linearized constant of the motion in a modified betatron with torsatron windings is given by

$$K_o = q_1 \left(\frac{X}{r_o}\right)^2 + q_2 \left(\frac{Z}{r_o}\right)^2 - \frac{2\delta P_\theta}{m r_o^2 \Omega_{zo}} \left(\frac{X}{r_o}\right), \qquad (1)$$

where

$$q_1 = 1 - n + n_t - n^* + 2\langle P_\theta \rangle / m r_o^2 \Omega_{zo}, \quad q_2 = n + n_t - n^*,$$

$$K_o = -\frac{2\delta P_\theta}{m r_o^2 \Omega_{zo}}, \qquad n_t = \frac{(\Omega_{so}^{ex} \varepsilon_t)^2 r_o \alpha}{2\Omega_{zo}(-\hat{\Omega}_{\theta o} + \beta_{\theta o} \gamma_o \omega_{wo})}$$

is the torsation field index, $n^* = 2\nu r_o c/(\gamma_o^2 a^2 \beta_{\theta o} \Omega_{zo})$ and $\hat{\Omega}_{\theta o} < 0$ is

the combined toroidal field at r_o. The rest of the parameters are defined in Ref. 10.

For stellarator windings the coefficient $\mathcal{Q}_{so}^{ex}\ \varepsilon_s = 2\mathcal{Q}_{so}^{ex}\ \varepsilon_t$ and therefore, for the same current in the windings, the stellarator field index becomes

$$n_s = \frac{4(\mathcal{Q}_{so}^{ex}\ \varepsilon_t)^2\ r_o \alpha}{2\mathcal{Q}_{zo}\ (\mathcal{Q}_{so}^{ex} + \beta_{\theta o}\gamma_o\ \omega_{wo})} . \qquad (2)$$

In Eq. (2) we have replaced $-\hat{\mathcal{Q}}_{\theta o} = \mathcal{Q}_{so}^{ex}$ since the zero order toroidal magnetic field generated by the stellarator windings is zero. Equation (1) can be written as

$$\left[\sqrt{q_1}\ \frac{X}{r_o} + \frac{K_o}{2\sqrt{q_1}}\right]^2 + q_2 \left(\frac{Z}{r_o}\right)^2 = K_o \left(1 + K_o/4\ q_1\right),$$

and therefore the displacement of the center of the orbit ΔX from the minor axis is

$$\frac{\Delta X}{r_o} = -\frac{K_o}{2q_1} = \frac{2\ \delta P_\theta\ /\ m\ r_o^2\ \mathcal{Q}_{zo}}{1 - n + n_s - n^* + 2\ \langle P_\theta \rangle\ /\ m r_o^2\ \mathcal{Q}_{zo}} . \qquad (3)$$

Since the coefficient $\mathcal{Q}_{so}^{ex}\ \varepsilon_s$ is proportional to the current flowing in the stellarator windings, as the winding current increases, n_s increases until q_1 (q_1 is less than q_2 for n=0.5) becomes zero. At this value of the winding current the curve of Fig. 6 becomes vertical. For even higher values of the current the reference electron at the ring centroid behaves like a single particle. This is manifested by the negative slope of the curves for 20 and 30 kA.

The curve for 30 kA in Fig. 6 has been truncated at $B_z = 0$ because we are interested only in the useful bandwidth of the device. Actually, the 30 kA curve intersects the outer wall of the torus at $B_{zo} = -55$ Gauss.

Figure 7 shows δ vs. B_{zo} for three values of the current when the opening in the windings is 4 cm wide. This opening is centered around z=0. A new feature appears in this figure that was not present in Fig. 6. Both the 20 and 30 kA curves stop considerably short of the outer wall and the 20 kA curve does not reach the inner wall. Within the range of the parameters considered, we have not found stable orbits in these regions. The ring centroid orbits change from stable to unstable with very small change in the value of the vertical magnetic field.

Figures 8 and 9 show δ vs. B_{zo} with a 4 cm wide gap and without a gap for 10 and 20 kA winding current. It appears that in the space charge dominated regime (Fig. 8) the gap slightly increases the bandwidth of the device. However, in the single particle regime (Fig. 9) the gap always reduces the bandwidth.

Figure 10 shows δ vs. B_{zo} for 0, 4 and 8 cm wide gaps when the current in the windings is 30 kA. It is apparent from these results that the bandwidth of the device is reduced as the width of the gap increases. For a 4 cm gap the ring equilibrium position is located on the minor axis when $B_{zo} = 50$ G. Therefore, the fractional bandwidth of the device is $\Delta B_z/B_{zo} = (67-5)/50 = 1.3$ or 130%, which is more than sufficient.

Table II summarizes the useful bandwidth of the various configurations that have been presented in this report. The negative values of ΔB_z correspond to space charge dominated equilibrium, i.e. when both q_1 and q_2 are negative. However, during acceleration n* is reduced and thus the ring has to cross the instability gap and probably will be lost.

III. Conclusions

We have developed two strong focusing field configurations that provide high midplane accessibility and therefore are compatible with presently contemplated extraction schemes from high current, toroidal accelerators. Although the useful bandwidth of these configurations is smaller than the bandwidth of the non-split stellatron, it is more than sufficient even for modest (20-30 kA) winding current.

Table I: Various Parameters Common to all runs in Figs. 6-10

Total beam energy (diode) γ_d	= 3.35
Beam kinetic energy γ	= 1.75
Beam radius r_b	= 1.0 cm
Beam current	= 4.92 kA
Torus major radius r_o	= 100 cm
Torus minor radius a	= 16 cm
Stellarator winding radius	= 20 cm
Stellarator winding period	= 157 cm
Centroid position at injection	= 106 cm
Toroidal magnetic field at r_o, $z = 0$, $B_{\theta o}$	= -5000 Gauss
External field index n	= 0.5

Table II: Summary of Useful Bandwidths for Figs. 6-10

Winding Current (kA)	Gap (cm)	B_{zo} injection (Gauss)	B_{zo} inner wall (Gauss)	Bandwidth ΔB_z (Gauss)
0	0	50	74	-24
10	0	52	66	-14
10	4	53	68	-16
20	0	58	43	+15
20	4	60	48	+12
30	0	62	5	+57
30	4	68	22	+46
30	8	71	38	+33

References

1. P. Sprangle and C. A. Kapetanakos, J. Appl. Phys. 119, (1978).
2. C. A. Kapetanakos, P. Sprangle, D. P. Chernin, S. J. Marsh, and I. Haber, Phys. Fluids 26, 1634 (1983).
3. D. Chernin and P. Sprangle, Part. Accel. 12, 85 (1982).
4. W. Manheimer and J. Finn, Part. Accel. 14, 29 (1983).
5. C. A. Kapetanakos, S. J. Marsh, Phys. Fluids 28, 2263 (1985).
6. J. M. Grossman, T. M. Finn, and W. Manheimer, Phys. Fluids 29, 695 (1985).
7. G. Barok and N. Rostoker, Phys. Fluids 26, 856 (1983).
8. H. S. Uhm, R. C. Davidson, and J. Petillo, Phys. Fluids 28, 2537 (1985).
9. C. W. Roberson, A. Mondelli, and D. Chernin, Phys. Rev. Letts. 50, 507 (1983).
10. C. A. Kapetanakos, D. Dialetis, and S. J. Marsh, Part. Accel. 21, 1 1987; NRL Memo Report No. 5619 (1985).
11. C. A. Kapetanakos, D. Dialetis, and S. J. Marsh, Proc. of the Conference on the Application of Accelerators in Research and Industry, Denton, TX, Nov. 1986, Nucl. Instrum. and Methods in Phys. Res. B24, 805 (1987).
12. P. Sprangle and C. A. Kapetanakos, Part. Accel. 18, 203 (1986).

NRL Modified Betatron

Strong Focusing Windings Compatible with Extraction

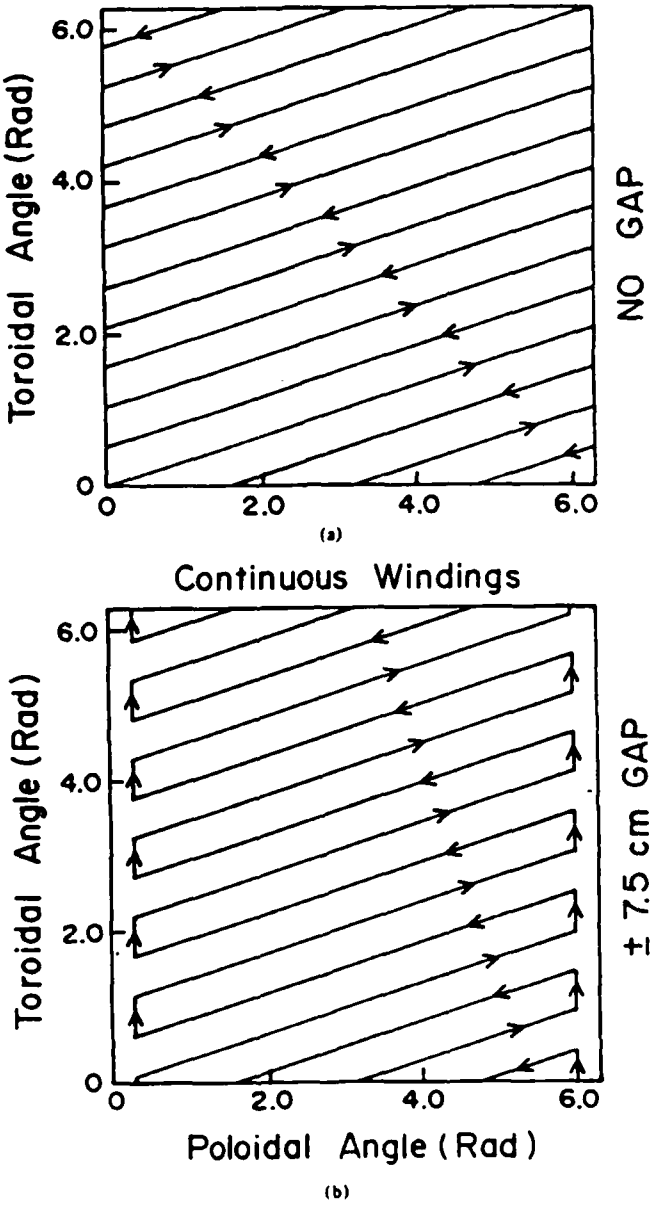

Fig. 1: Toroidal angle θ, poloidal angle ϕ plane for a three period stellarator winding. 1a shows the unsplit stellarator windings and 1b shows the split windings in the continuous current configurations. The windbacks are not shown in this figure.

NRL Modified Betatron

Strong focusing windings with high midplane accessibility for extraction

Continuous winding

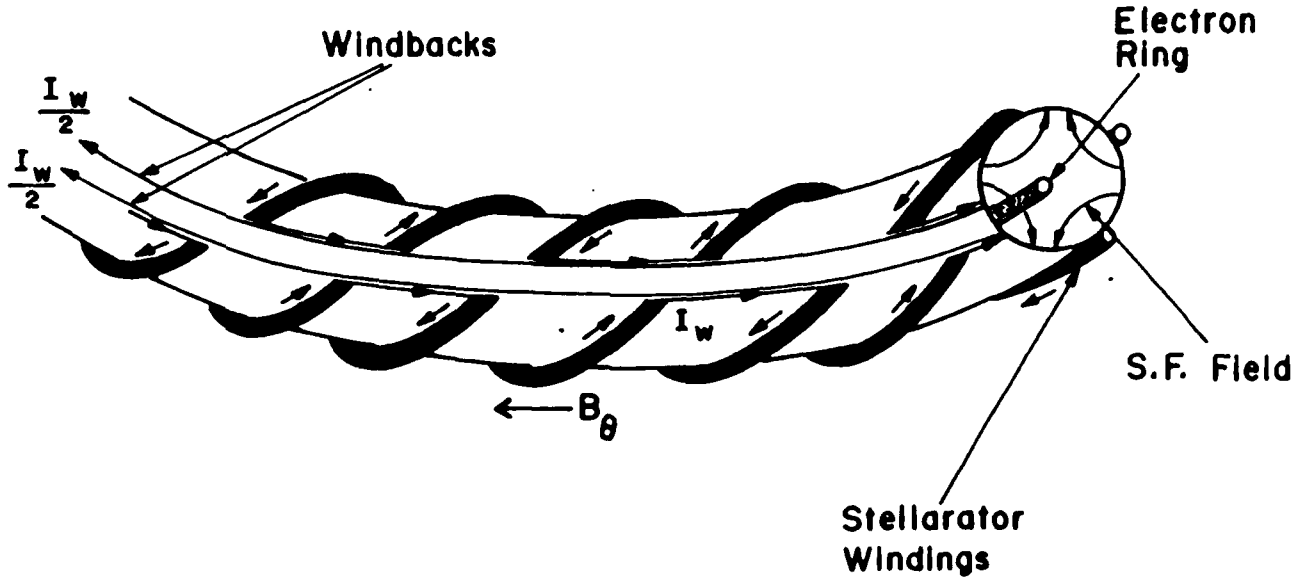

Fig. 2: Schematic of the split windings in the continous current configuration. Although this figure shows lefthanded windings all the calculations have been performed for right handed systems.

NRL Modified Betatron

Strong Focusing Windings Compatible with Extraction

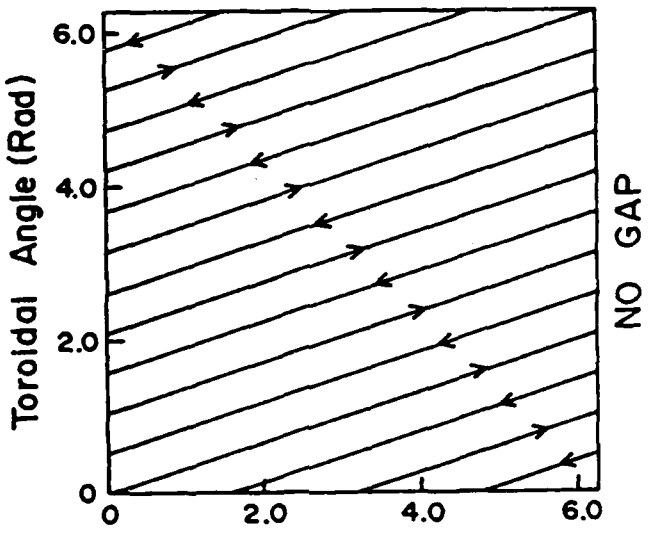

(a)

Modular

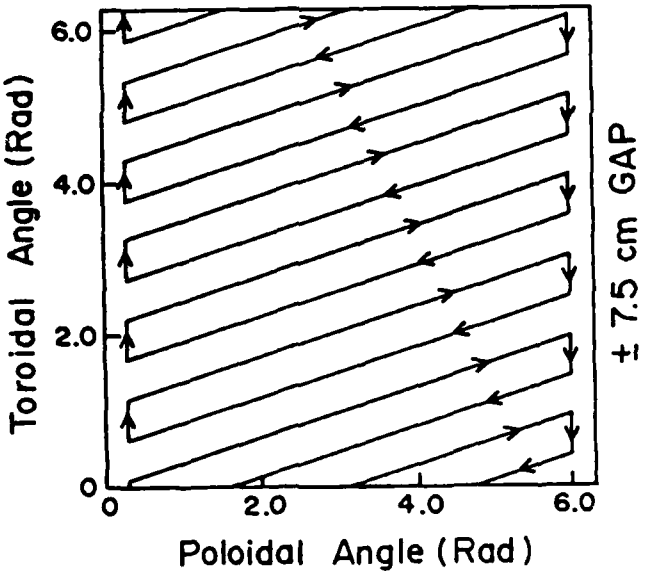

(b)

Fig. 3: Toroidal angle θ, poloidal angle ϕ plane for a three period stellarator winding. 3a shows the unsplit stellarator windings and 3b shows the split windings in the modular configuration. The windbacks run along the jumpers but are not shown in this Figure.

NRL Modified Betatron

Strong focusing windings with high midplane accessibility for extraction

Modular winding

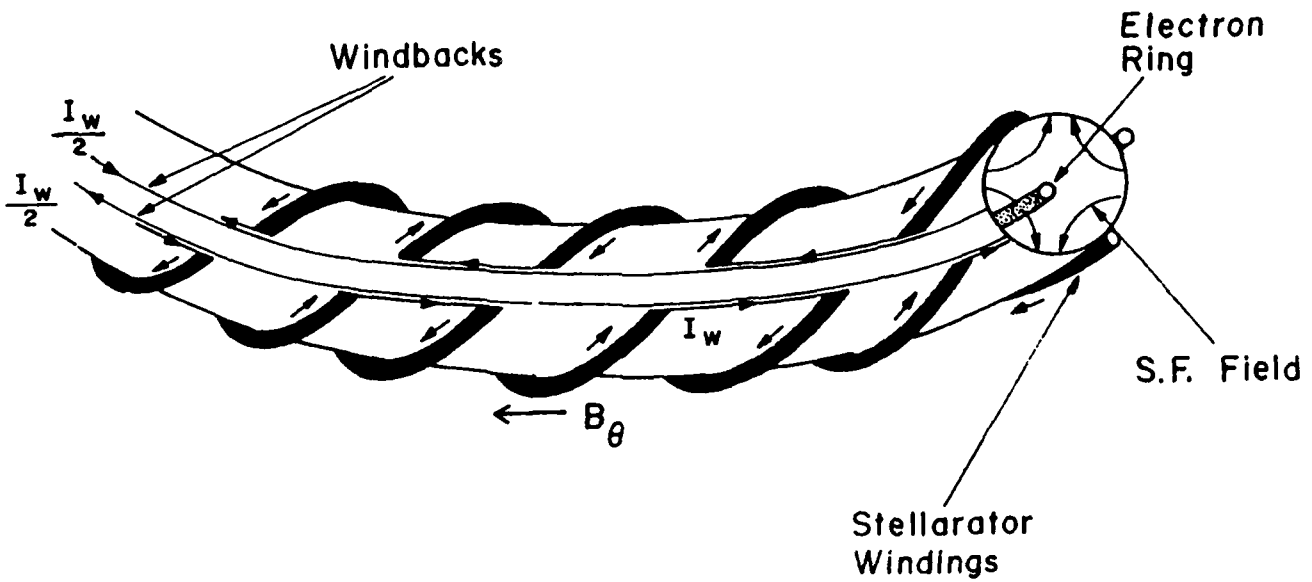

Fig. 4: Schematic of the split windings in the modular configuration.

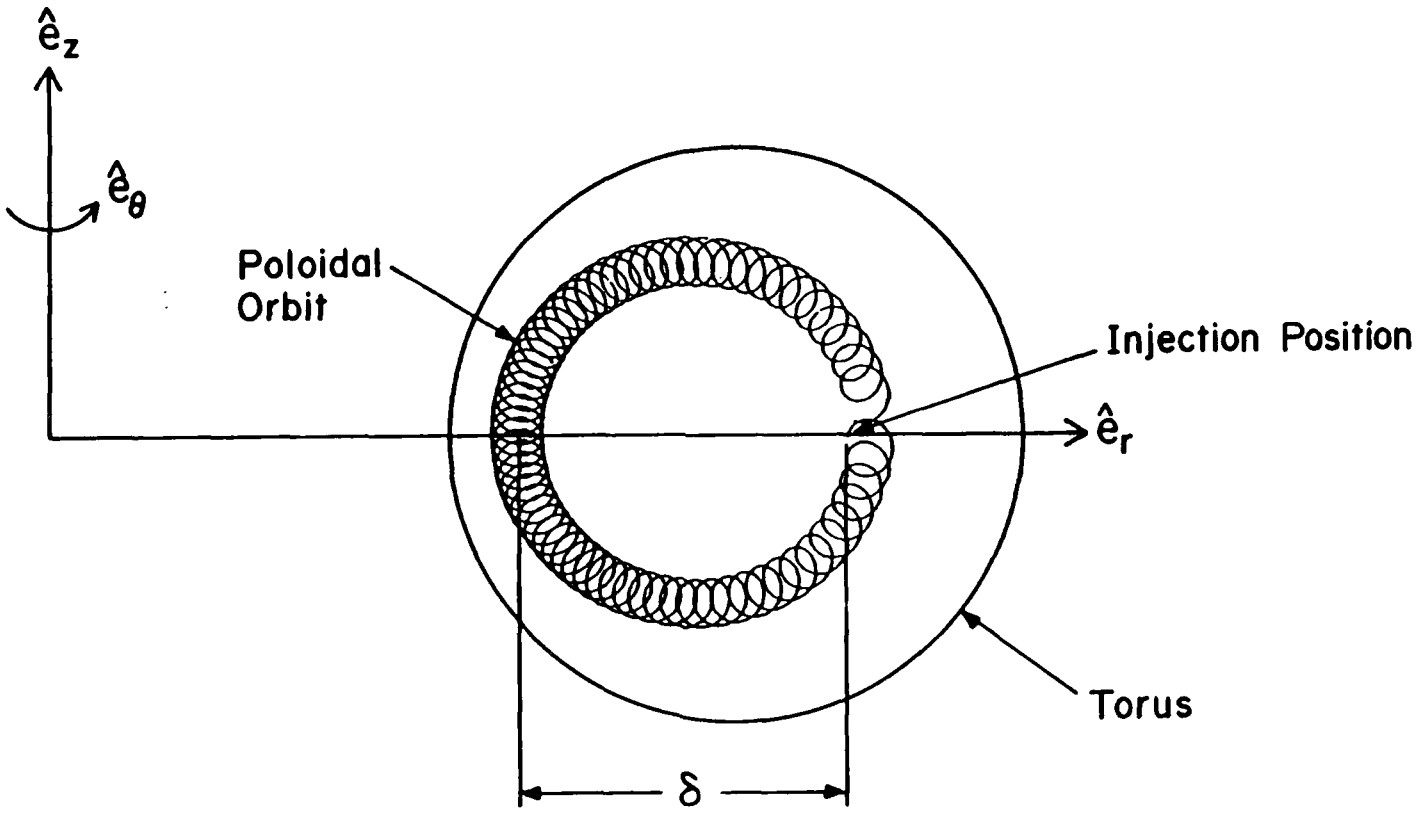

Fig. 5: System of coordinates and macroscopic (centroid) ring orbit in the transverse plane.

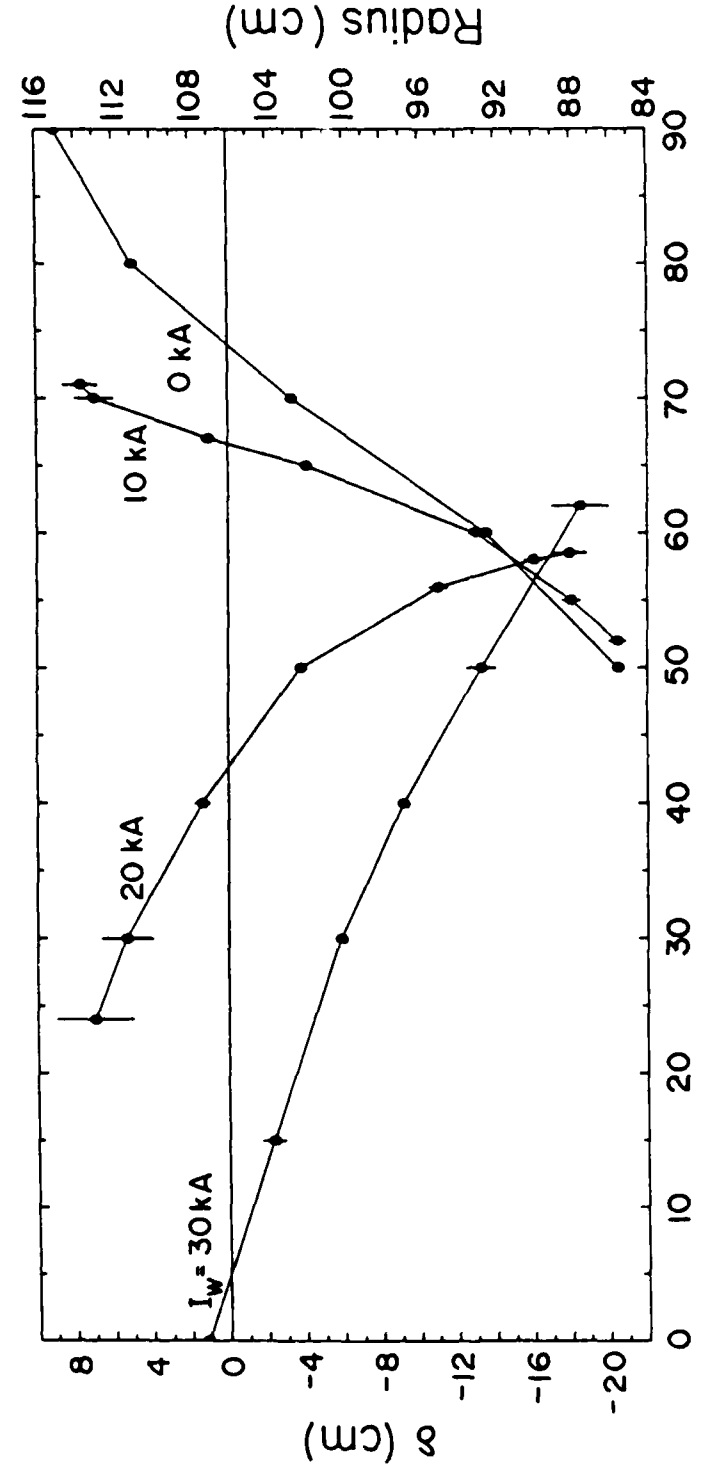

Fig. 6: Radial dimension δ of the macroscopic ring orbit in the transverse plane as a function of the vertical magnetic field B_{z0} for a modified betatron with conventional (unsplit) stellarator windings.

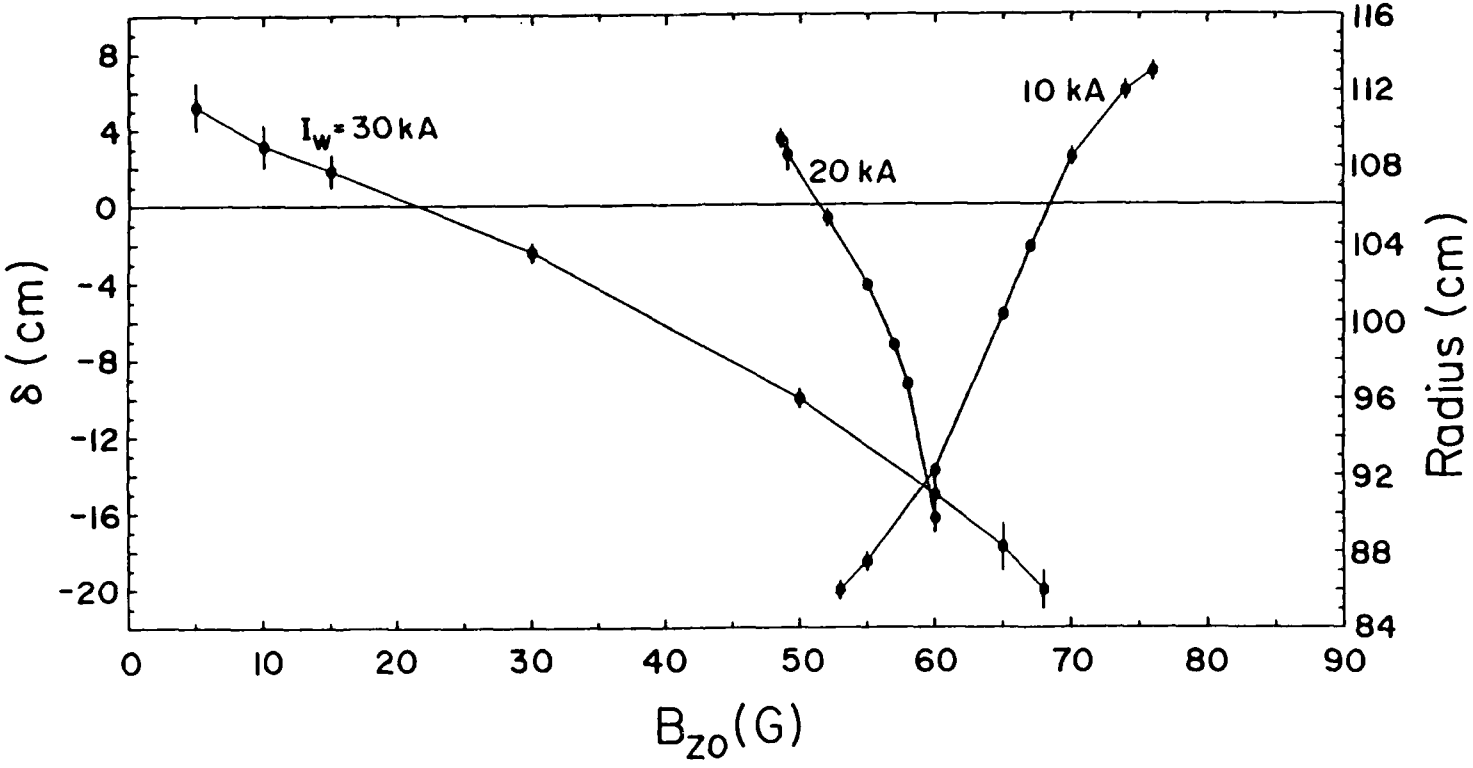

Fig. 7: Radial dimension δ of the macroscopic ring orbit in the transverse plane as a function of the vertical magnetic field B_{zo} for a modified betatron with a 4 cm gap strong focusing modular windings. The results of the continuous windings are very similar.

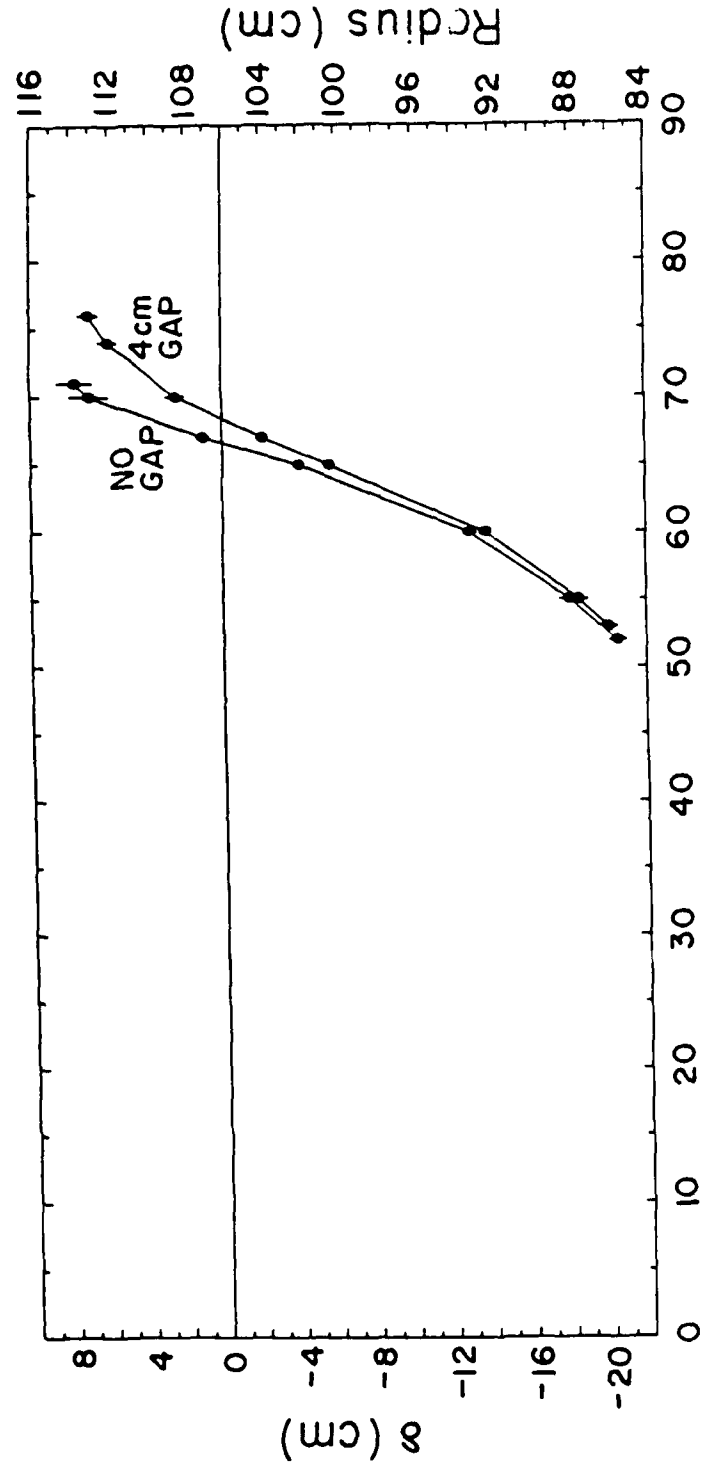

Fig. 8: Variation of δ with B_{ZO} for 0 and 4 cm gap windings. These results have been obtained with 10 kA winding current.

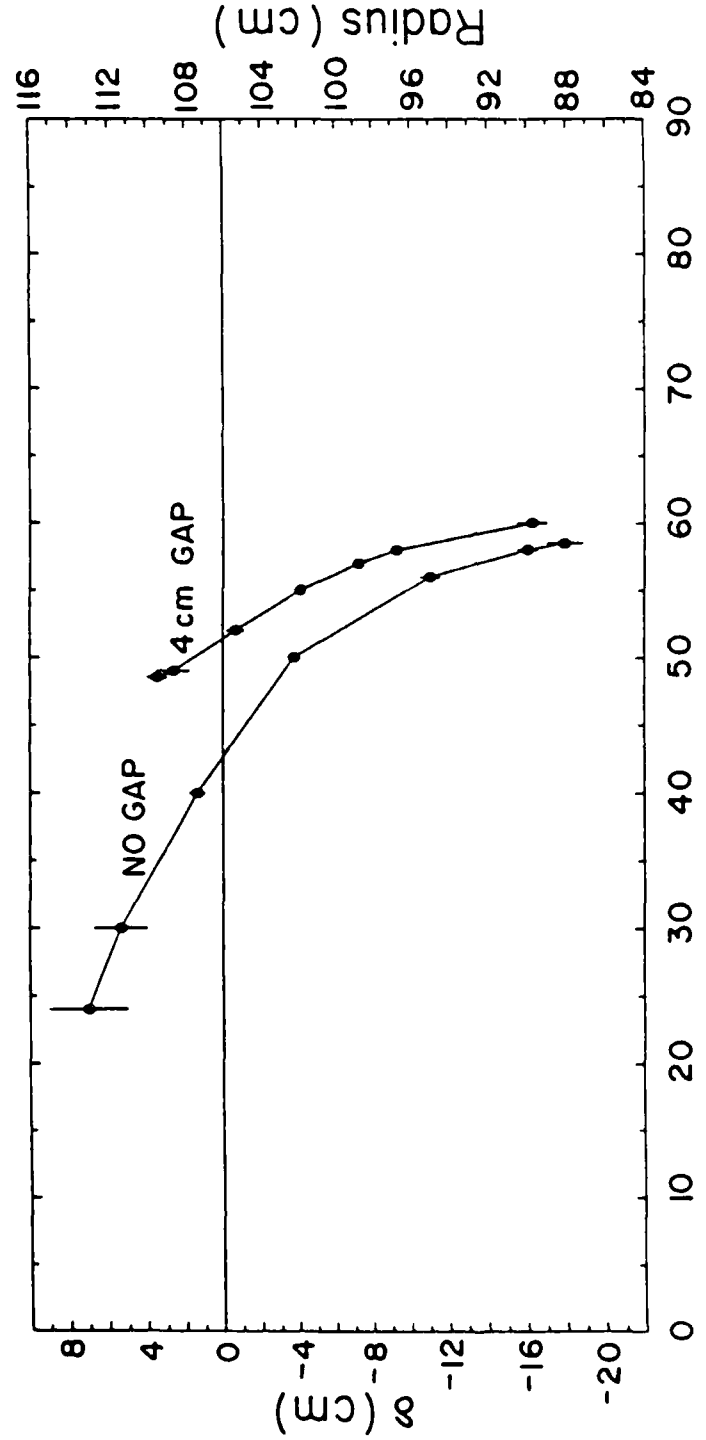

Fig. 9: As in Fig. 8 but with 20 kA winding current.

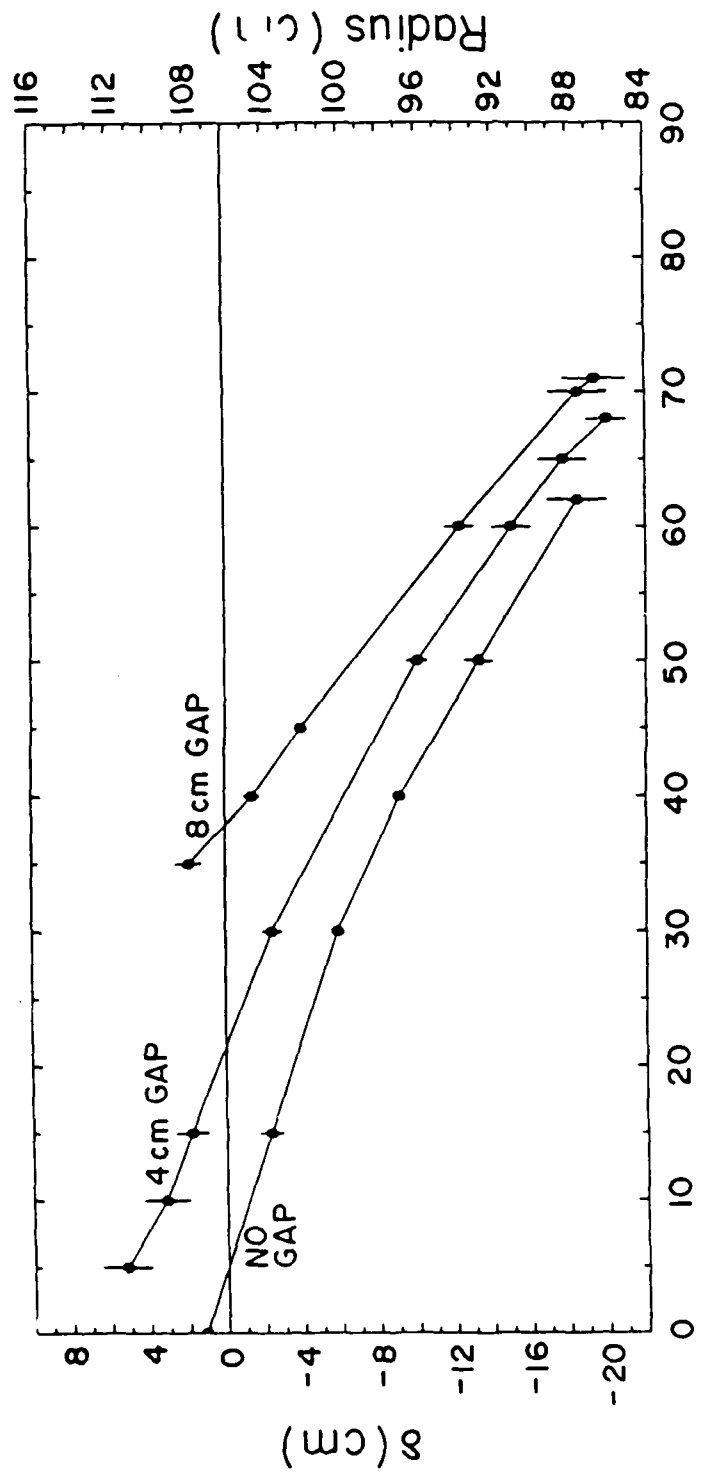

Fig. 10: Comparison of δ for three systems with 0, 4, and 8 cm gap windings. The current in the main windings is 30 kA.

DISTRIBUTION LIST
(Revised April 1987)

Dr. M. Allen
Stanford Linear Accelerator Center
Stanford, CA 94305

Dr. W. Barletta
Lawrence Livermore National Laboratory
P.O. Box 808
Livermore, CA 94550

Dr. M. Barton
Brookhaven National Laboratory
Upton, L.I., NY 11101

CDR William F. Bassett
APM for Test Systems Engineering
Naval Sea Systems Command, Code PMS-405
Washington, DC 20362-5101

Dr. Jim Benford
Physics International Co.
2700 Merced St.
San Leandro, CA 94577

Dr. Kenneth Bergerson
Plasma Theory Division - 5241
Sandia National Laboratories
Albuquerque, NM 87115

Dr. Daniel Birx
Lawrence Livermore National Laboratory
P.O. Box 808
Livermore, CA 94550

Dr. Charles Brau
Los Alamos Scientific Laboratory
Los Alamos, NM 87544

Dr. R. Briggs
Lawrence Livermore National Laboratory
P.O. Box 808
Livermore, CA 94550

Dr. Allan Bromborsky
Harry Diamond Laboratory
2800 Powder Mill Road
Adelphi, MD 20783

Dr. H. Lee Buchanan
Lawrence Livermore National Laboratory
P.O. Box 808
Livermore, CA 94550

Dr. M. Butram
Sandia National Laboratory
Albuquerque, NM 87115

Dr. M. Caponi
TRW Advance Tech. Lab.
I Space Park
Redondo Beach, CA 90278

Prof. F. Chen
Department of Electrical Engineering
University of California at Los Angeles
Los Angeles, CA 90024

Dr. D. Chernin
Science Applications Intl. Corp.
1710 Goodridge Drive
McLean, VA 22102

Dr. Charles C. Damm
Lawrence Livermore National Laboratory
P.O. Box 808
Livermore, CA 94550

Prof. R. Davidson
Plasma Fusion Center
M.I.T.
Cambridge, MA 02139

Dr. J. Dawson
University of California at Los Angeles
Department of Physics
Los Angeles, CA 90024

Dr. W.N. Destler
Department of Electrical Engineering
University of Maryland
College Park, MD 20742

Prof. W. Doggett
North Carolina State University
P.O. Box 5342
Raleigh, NC 27650

Dr. H. Dreicer
Director Plasma Physics Division
Los Alamos Scientific Laboratory
Los Alamos, NM 87544

Prof. W.E. Drummond
Austin Research Associates
1901 Rutland Drive
Austin, TX 78758

Dr. J.G. Eden
Department of Electrical Engineering
University of Illinois
155 EEB
Urbana, IL 61801

Dr. A. Faltens
Lawrence Berkeley Laboratory
Berkeley, CA 94720

Dr. T. Fessenden
Lawrence Livermore National Laboratory
P.O. Box 808
Livermore, CA 94550

Dr. A. Fisher
Physics Department
University of California
Irvine, CA 92664

Prof. H.H. Fleischmann
Laboratory for Plasma Studies and
School of Applied and Eng. Physics
Cornell University
Ithaca, NY 14850

Dr. T. Fowler
Associate Director
Magnetic Fusion Energy
Lawrence Livermore National Laboratory
P.O. Box 808
Livermore, CA 94550

Mr. George B. Frazier, Manager
Pulsed Power Research & Engineering Dept.
2700 Merced St.
P.O. Box 1538
San Leandro, CA 94577

LCDR W. Fritchie
APM for Test Systems Engineering
Naval Sea Systems Command, Code PMS-405
Washington, DC 20362-5101

Dr. S. Graybill
Harry Diamond Laboratory
2800 Powder Mill Road
Adelphi, MD 20783

Lt. Col. R. Gullickson
SDIO-DEO
Pentagon
Washington, DC 20301-7100

Dr. J.U. Guillory
JAYCOR
20550 Whiting St., Suite 500
Alexandria, VA 22304

Dr. Z.G.T. Guiragossian
TRW Systems and Energy RI/1070
Advanced Technology Lab
1 Space Park
Redondo Beach, CA 90278

Prof. D. Hammer
Laboratory of Plasma Physics
Cornell University
Ithaca, NY 14850

Dr. David Hasti
Sandia National Laboratory
Albuquerque, NM 87115

Dr. C.E. Hollandsworth
Ballistic Research Laboratory
DRDAB - BLB
Aberdeen Proving Ground, MD 21005

Dr. C.M. Huddleston
ORI
1375 Piccard Drive
Rockville, MD 20850

Dr. S. Humphries
University of New Mexico
Albuquerque, NM 87131

Dr. Robert Hunter
9555 Distribution Ave.
Western Research Inc.
San Diego, CA 92121

Dr. J. Hyman
Hughes Research Laboratory
3011 Malibu Canyon Road
Malibu, CA 90265

Prof. H. Ishizuka
Department of Physics
University of California at Irvine
Irvine, CA 92664

Dr. D. Keefe
Lawrence Berkeley Laboratory
Building 50, Rm. 149
One Cyclotron Road
Berkely, CA 94720

Dr. Donald Kerst
University of Wisconsin
Madison, WI 53706

Dr. Edward Knapp
Los Alamos Scientific Laboratory
Los Alamos, NM 87544

Dr. A. Kolb
Maxwell Laboratories
8835 Balboa Ave.
San Diego, CA 92123

Dr. Peter Korn
Maxwell Laboratories
8835 Balboa Ave.
San Diego, CA 92123

Dr. R. Linford
Los Alamos Scientific Laboratory
P.O. Box 1663
Los Alamos, NM 87545

Dr. C.S. Liu
Department of Physics
University of Maryland
College Park, MD

Prof. R.V. Lovelace
School of Applied and Eng. Physics
Cornell University
Ithaca, NY 14853

Dr. S.C. Luckhardt
Plasma Fusion Center
M.I.T.
Cambridge, MA 02139

Dr. John Madey
Physics Department
Stanford University
Stanford, CA 94305

Dr. J.E. Maenchen
Division 1241
Sandia National Lab.
Albuquerque, NM 87511

Prof. T. Marshall
School of Engineering and Applied Science
Plasma Laboratory
S.W. Mudd Bldg.
Columbia University
New York, NY 10027

Dr. M. Mazarakis
Sandia National Laboratory
Albuquerque, NM 87115

Dr. D.A. McArthur
Sandia National Laboratories
Albuquerque, NM 87115

Prof. J.E. McCune
Dept. of Aero. and Astronomy
M.I.T.
77 Massachusetts Ave.
Cambridge, MA 02139

Dr. J. McNally, Jr.
Oak Ridge National Lab.
P.O. Box Y
Oak Ridge, TN 37830

Prof. G.H. Miley, Chairman
Nuclear Engineering Program
214 Nuclear Engineering Lab.
Urbana, IL 61801

Dr. Bruce Miller
Sandia National Laboratory
Albuquerque, NM 87115

Dr. A. Mondelli
Science Applications, Inc.
1710 Goodridge Drive
McLean, VA 22102

Dr. Phillip Morton
Stanford Linear Accelerator Center
Stanford, CA 94305

Dr. M. Nahemov
Westinghouse Electric Corporation
1310 Beutah Rd.
Pittsburg, PA 15235

Prof. J. Nation
Lab. of Plasma Studies
Cornell University
Ithaca, NY 14850

Dr. V.K. Neil
Lawrence Livermore National Laboratory
P.O. Box 808
Livermore, CA 94550

Dr. Gene Nolting
Naval Surface Weapons Center
White Oak Laboratory
10901 New Hampshire Ave.
Silver Spring, MD 20903-5000

Dr. C.L. Olson
Sandia Laboratory
Albuquerque, NM 87115

Dr. Arthur Paul
Lawrence Livermore National Laboratory
P.O. Box 808
Livermore, CA 94550

Dr. S. Penner
National Bureau of Standards
Washington, D.C. 20234

Dr. Jack M. Peterson
Lawrence Berkeley Laboratory
Berkeley, CA 94720

Dr. R. Post
Lawrence Livermore National Lab.
P.O. Box 808
Livermore, CA 94550

Dr. Kenneth Prestwich
Sandia National Laboratory
Albuquerque, NM 87115

Dr. S. Prono
Lawrence Livermore National Lab.
P.O. Box 808
Livermore, CA 94550

Dr. Sid Putnam
Pulse Science, Inc.
600 McCormick Street
San Leandro, CA 94577

Dr. Louis L. Reginato
Lawrence Livermore National Lab
P.O. Box 808
Livermore, CA 94550

Prof. N. Reiser
Dept. of Physics and Astronomy
University of Maryland
College Park, MD 20742

Dr. M.E. Rensink
Lawrence Livermore National Lab
P.O. Box 808
Livermore, CA 94550

Dr. D. Rej
Lab for Plasma Physics
Cornell University
Ithaca, NY 14853

Dr. J.A. Rome
Oak Ridge National Lab
Oak Ridge, TN 37850

Prof. Norman Rostoker
Dept. of Physics
University of California
Irvine, CA 92664

Dr. J. Sazama
Naval Surface Weapons Center
Code 431
White Oak Laboratory
Silver Spring, MD 20910

Prof. George Schmidt
Physics Department
Stevens Institute of Tech.
Hoboken, NJ 07030

Philip E. Serafim
Northeastern University
Boston, MA 02115

Dr. Andrew Sessler
Lawrence Berkeley National Lab
Berkeley, CA 94720

Dr. John Siambis
Lockheed
Palo Alto Research Lab
3257 Hanover Street
Palo Alto, CA 94304

Dr. Adrian C. Smith
Lawrence Livermore National Laboratory
P.O. Box 808
Livermore, CA 94550

Dr. Lloyd Smith
Lawrence Berkeley National Laboratory
Berkeley, CA 94720

Dr. A. Sternlieb
Lawrence Berkely National Laboratory
Berkeley, CA 94720

Dr. D. Straw
W.J. Schafer Assoc.
2000 Randolph Road, S.E., Suite A
Albuquerque, NM 87106

Prof. C. Striffler
Dept. of Electrical Engineering
University of Maryland
College Park, MD 20742

Prof. R. Sudan
Laboratory of Plasma Studies
Cornell University
Ithaca, NY 14850

Dr. W. Tucker
Sandia National Laboratory
Albuquerque, NM 87115

Dr. H. Uhm
Naval Surface Weapons Center
White Oak Laboratory
10901 New Hampshire Ave. Code R41
Silver Spring, MD 20903-5000

Dr. William Weldon
University of Texas
Austin, TX 78758

Dr. Mark Wilson
National Bureau of Standards
Washington, DC 20234

Dr. P. Wilson
Stanford Linear Accelerator Center
Stanford, CA 94305

Prof. C.B. Wharton
303 N. Sunset Drive
Ithaca, NY 14850

West Defense Technical Information Center - 2 copies

NRL Code 2628 - 20 copies

NRL Code 4700 - 26 copies

NRL Code 4710 - 40 copies

MAILING LIST/FOREIGN

Library
Institut fur Plasmaforschung
Universitat Stuttgart
Pfaffenwaldring 31
7000 Stuttgart 80, West Germany

Ken Takayama
KEN, TRISTAN Division
Oho, Tsukuba, Ibaraki, 305 JAPAN

END

12-87

DTIC